Paper:

Virtual Driving Simulator for Measuring Dynamic Properties of Human Arm Movements

Yoshiyuki Tanaka*, Ryoma Kanda*, Naoki Yamada, Hitoshi Fukuba**, Ichiro Masamori**, and Toshio Tsuji***

*Department of Artificial Complex Systems Engineering, Hiroshima University
1-4-1 Kagamiyama, Higashi-hiroshima, Hiroshima 739-8527, Japan
E-mail: ytanaka@bsys.hiroshima-u.ac.jp
**Mazda Motor Corporation
3-1 Shinchi, Fuchu-cho, Aki-gun, Hiroshima 730-8670, Japan
[Received November 21, 2005; accepted January 26, 2006]

This paper presents a virtual driving simulator using robotic devices as an example of human-machine systems to investigate dynamic properties of human movements in the operation of drive interfaces, such as steering wheels and transmission shifters. The simulator has virtual steering and transmission systems under variable impedance control, providing the operators with realistic operational response. Mechanical impedance parameters around the steering rotational axis were measured to demonstrate the effectiveness of the developed simulator.

Keywords: mechanical impedance, man-machine system, variable impedance control

1. Introduction

A human can maneuver many different mechanical systems by naturally and effectively changing posture and dynamic properties of movements according to a target task. When operating a vehicle in the streets, for example, drivers vary the positioning and pressure of arm movement on the steering wheel and the shifter to comply with speed and steering needs. Human drivers adapt their movements to the mechanical properties of the drive interfaces. If such interfaces modified their dynamics according to dynamic properties of driver's movements, drivers would operate their vehicles more comfortably and effectively. To develop intelligent interfaces for mechanical systems, dynamic properties of human movements operating the interfaces should be analyzed.

Such dynamic properties of human movements can be expressed in mechanical impedance parameters, i.e., stiffness, viscosity, and inertia. Many experimental studies on human hand impedance in multi-joint arm movements have been reported. Mussa-Ivaldi et al. [1], for example, pioneered the measurement of human hand impedance and examined hand stiffness in a stable arm posture. They found that hand stiffness strongly depends on arm posture, and that a human can change the size of a stiffness ellipse, although he/she can change neither its orientation nor its shape. Research by Dolan et al. [2] and Tsuji et al. [3–5] on hand stiffness, viscosity, and inertia verified a qualitative parallel between hand stiffness and viscosity. Tsuji et al. [4] also showed that human hand viscoelastic properties are widely affected by muscle activation level during isometric contraction in the upper limb. Gomi and Kawato [6] documented hand stiffness in reaching movements, reporting that hand stiffness changes more considerably during reaching movements than when individuals maintained a particular arm posture. These studies examined human impedance properties during single-arm movements in which the arm configuration is restricted on the horizontal plane or the vertical plane.

Constructing human-machine systems using impedance-controlled robots [7] has been discussed in robotics [8–13]. The basic concept is that robot impedance properties ensure overall stability and maneuverability for human operators based on human impedance. Ikeura et al. [12, 13], for example, proposed variable-impedance control that switches robot impedance properties during a task. They also supposed that the maneuverability of a human-machine system could be improved by implementing human impedance, which was measured in the target task with two human operators, into impedance-controlled robots. Yamada et al. [11, 14] developed skill assistance that varies robot impedance properties according to human movements to perform iterative tasks at constant speed and high quality. These previous studies focus on mainly a design approach of robot impedance properties without considering dynamic properties of operator's movements. Recently, Ikeura et al. [15, 16] developed the steering system using an impedance-controlled robot, reporting the close relationship between operational sensibilities and human hand stiffness measured during dual-arm steering. They did not estimate the accuracy of human hand impedance or deal with shifting in the developed system.

In this paper, a virtual driving simulator using robotic

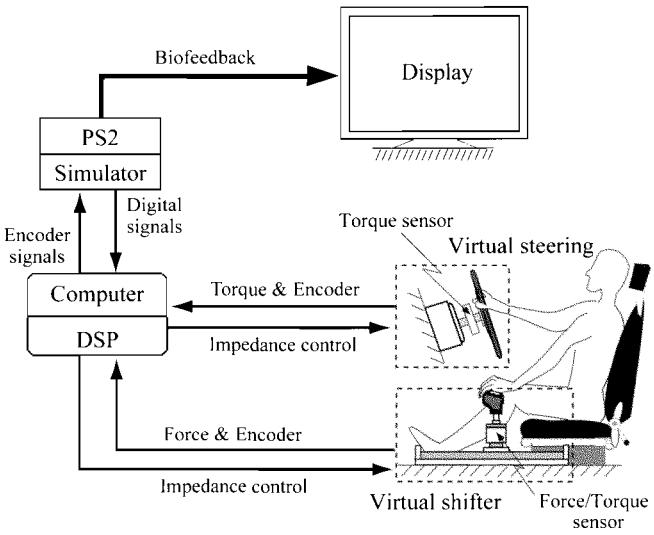

(a)

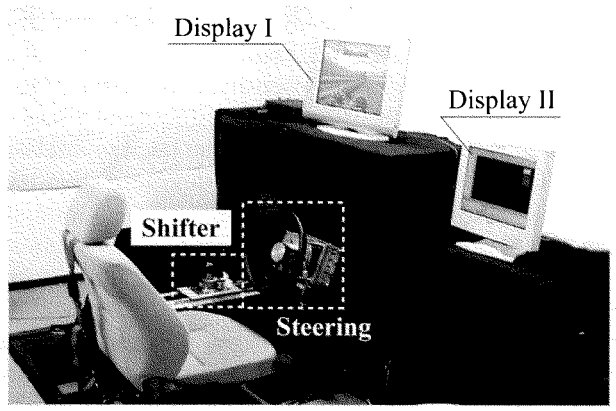

(b)

Fig. 1. Virtual driving simulator.

devices is developed to investigate dynamic properties of human arm movements during the operations of drive interfaces. The simulator utilizes a virtual steering system and a virtual transmission shifter system under variable impedance control and provides operational force feedback to the operator.

This paper is organized as follows: Section 2 describes the developed virtual driving simulator, and Section 3 explains how to measure human arm impedance during virtual steering. Section 4 discusses a series of experiments with different viscoelastic patterns in the developed simulator, presenting examples of estimated human arm impedance according to rotational angle of the steering wheel.

2. Virtual Driving Simulator

2.1. System Configuration

Figure 1 diagrams the developed virtual driving simulator. The simulator consists of robots providing force feedback to human operators and measuring mechanical impedance properties of human movements in virtual steering and shifting, the computer for controlling the robots, and the display to feedback visual information to operators.

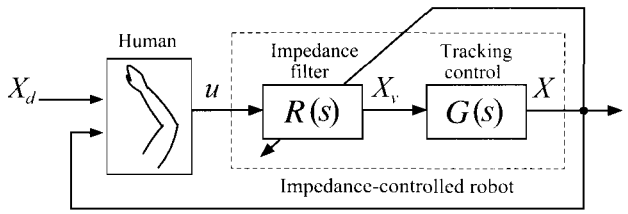

Fig. 2. A block diagram of the control system implementing the virtual driving simulator.

Virtual steering system includes a direct-drive motor (NSK, Ltd., maximum torque ±20Nm). A steering wheel (NARDI, Ltd., diameter: 0.37m) and a rotation torque sensor (Sohgohkeiso Corp., maximum toque 50N·m) are installed on the rotating part of the motor. The rotation angle of the steering wheel is measured by an encoder in the motor (encoder resolution: 51,200 pulse/r). The virtual transmission shifter has a direct-drive liner motor table with one degree of freedom (Nihon Thomson Corp., maximum force ±10kgf), focusing on shifting from Low to 2nd gear. A shift knob and six-axis force/torque sensor (NITTA, Ltd., resolution ability: force x axis, y axis: 6.1×10^{-3}N, z axis: 1.2×10^{-2}N, torque: 1.1×10^{-3}Nm) are installed on the moving part of the linear motor table. The hand position is measured by an encoder in the motor table (encoder resolution: 2μm). Robots in the simulator are controlled by a DSP board (dSPACE : ds1104) that provides stable control and high-quality data measurement in high sampling (2kHz).

The virtual driving display consists two liquid crystal displays: Display I provides the run situation, according to the rotational angle of the steering wheel and the shift position, created by a graphics simulator (Playstation2, Sony Computer Entertainment Inc.); and Display II measured data during operations of the virtual steering and the virtual transmission shifter.

2.2. Control System

Robotic devices in the driving simulator are controlled by impedance control (See **Fig.2**). Robots move following virtual target point X_v calculated from impedance filter $R(s)$ with control input u generated by the human operator.

In the developed driving simulator, dynamic properties of virtual steering can be represented as follows:

$$M_\theta \ddot{\theta}_v + B_\theta(\theta)\dot{\theta}_v + K_\theta(\theta)(\theta_v - \theta_c) = T \quad . \quad . \quad . \quad (1)$$

where M_θ is the inertia of a virtual steering system; $B_\theta(\theta)$ and $K_\theta(\theta)$ variable viscosity and stiffness as a function of the rotational angle of steering wheel θ, respectively; θ_c equilibrium for $K(\theta)$; and T the steering torque generated by the human operator.

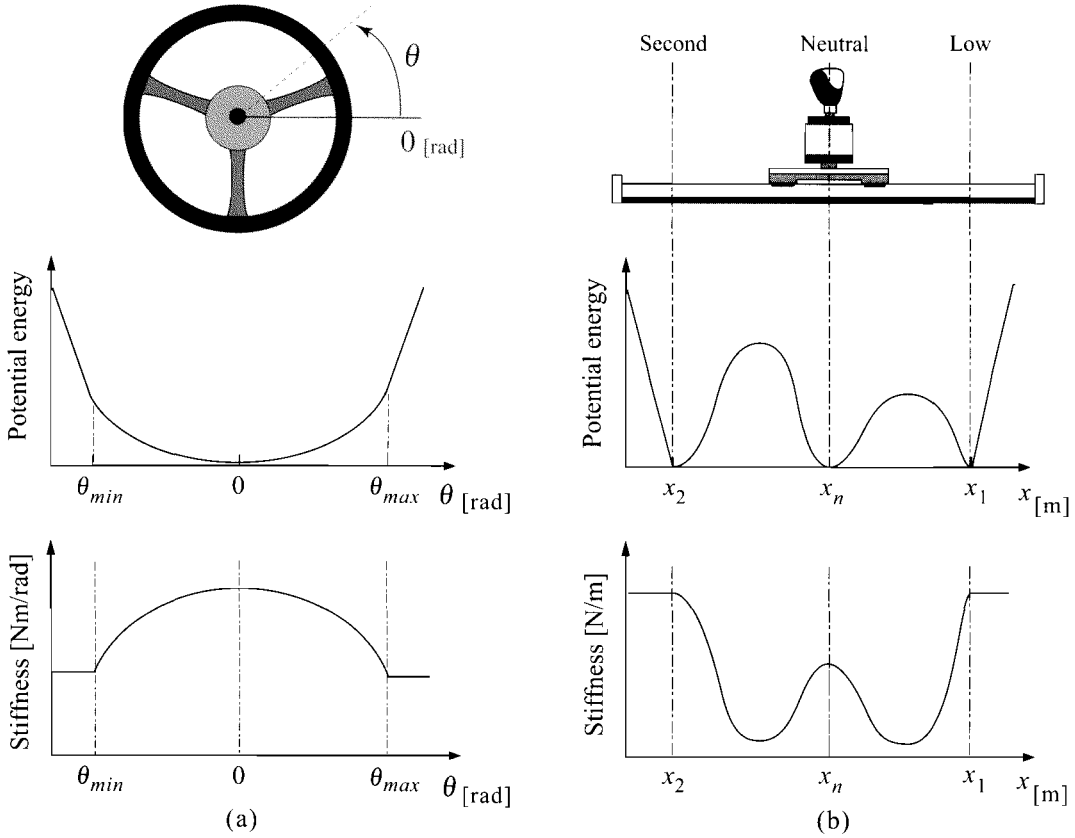

Fig. 3. Design of viscoelastic patterns for virtual driving simulator.

Dynamic properties of the virtual transmission shifter can be expressed as follows:

$$M\ddot{x}_v + B(x)\dot{x}_v + K(x)(x_v - x_c) = F \quad \ldots\ldots \quad (2)$$

where M is the inertia of a virtual shift; $B(x)$ and $K(x)$ variable viscosity and stiffness as a function of the hand position x; x_c equilibrium for $K(x)$; and F hand force generated by the operator.

Considering characteristics of general steering interfaces, $\theta = 0$ rad can be selected as equilibrium θ_c for stiffness effects in virtual steering. Therefore, the profile of potential energy and an appropriate stiffness pattern for θ during steering can be drawn as shown in **Fig.3(a)**. In this paper, viscoelastic patterns are modeled for θ by a third-order polynomial as

$$K_\theta(\theta) = \alpha_0 + a_1\theta + \alpha_2\theta^2 + \alpha_3\theta^3 \quad \ldots\ldots \quad (3)$$

$$B_\theta(\theta) = \beta_0 + \beta_1\theta + \beta_2\theta^2 + \beta_3\theta^3 \quad \ldots\ldots \quad (4)$$

where α_i and β_i $(i = 0, 1, \ldots, 3)$ are coefficients for determining viscoelastic patterns.

Regarding points of Low gear x_1, Neutral gear (N gear, here after) x_n, and 2nd gear x_2 as equilibrium x_c in virtual shifting (See **Fig.3(b)**), the profile of potential energy during shifting operations from Low to 2nd gear can be drawn as shown in the middle panel. As seeing in the bottom panel, a viscoelastic pattern in each interval of 3 gears is designed with Gaussian functions while equilibrium x_c

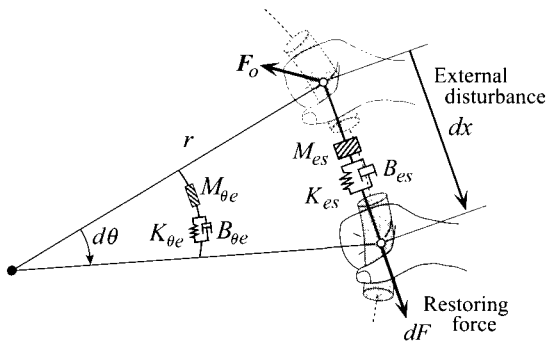

Fig. 4. Schematic description of hand impedance measurement.

is switched by the following rule [17]:

$$x_c = \begin{cases} x_1 & (x > x_{c1}) \\ x_n & (x_{c2} \le x \le x_{c1}) \\ x_2 & (x < x_{c2}) \end{cases} \quad \ldots\ldots \quad (5)$$

where x_{c1} and x_{c2} represent switching points of equilibrium.

Implementing an appropriate viscoelastic pattern in impedance control in robotic devices, the developed simulator provides realistic operational feelings for steering and shifting operations.

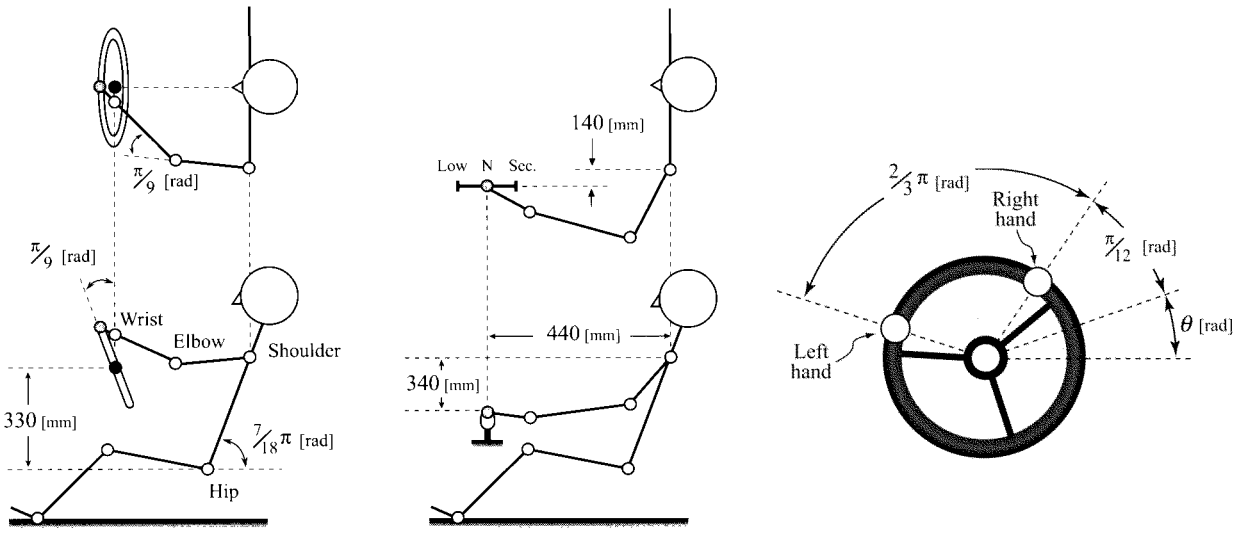

Fig. 5. Experimental conditions in virtual steering and shifting.

3. Impedance Measurement in Steering

This section details the measurement of human hand impedance contributing directly to steering, i.e., hand impedance tangential to the steering wheel with the developed virtual steering.

Consider multi-joint arm movements during steering in the l-dimensional task space. When the subject's endpoint is displaced from its equilibrium by a small disturbance with a short duration as shown in **Fig.4**, dynamic characteristics of the hand can be expressed with the following impedance model [3]:

$$\boldsymbol{M}_e\ddot{\boldsymbol{X}}(t)+\boldsymbol{B}_e\dot{\boldsymbol{X}}(t)+\boldsymbol{K}_e(\boldsymbol{X}(t)-\boldsymbol{X}_v(t))=-\boldsymbol{F}(t) \quad (6)$$

where $\boldsymbol{F}(t)\in\Re^l$ is hand force; $\boldsymbol{X}(t)\in\Re^l$ hand position; $\boldsymbol{X}_v(t)\in\Re^l$ a virtual trajectory; and $\boldsymbol{M}_e\in\Re^{l\times l}$, $\boldsymbol{B}_e\in\Re^{l\times l}$ and $\boldsymbol{K}_e\in\Re^{l\times l}$ hand inertia, viscosity, and stiffness. Assuming that disturbance dx is applied tangentially to the steering wheel at time t_0, dynamic characteristics of the human hand at time t tangentially can be described with restoration force dF from Eq.(6) as follows:

$$M_{es}d\ddot{x}(t)+B_{es}d\dot{x}(t)+K_{es}dx(t)=-dF(t) \quad (7)$$

where M_{es}, B_{es} and K_{es} are hand inertia, viscosity, and stiffness tangentially to the steering wheel.

In rotational movements of the hand with radius r as shown in **Fig.4**, the norm of hand displacement dx can be approximated with rotational displacement around steering rotational axis $d\theta$ as

$$dx(t)\approx r\,d\theta(t) \quad (8)$$

and reaction torque around from the environment to hand $dT_e(t)$ is

$$dT_e(t)=r\,dF(t). \quad (9)$$

From Eqs.(7)-(9), mechanical impedance properties around the steering rotational axis can be expressed as

$$M_{\theta e}d\ddot{\theta}(t)+B_{\theta e}d\dot{\theta}(t)+K_{\theta e}d\theta(t)=-dT_e(t) \quad (10)$$

and mechanical impedance parameters by the single arm calculated by

$$M_{\theta e}=r^2M_{es} \quad (11)$$

$$B_{\theta e}=r^2B_{es} \quad (12)$$

$$K_{\theta e}=r^2K_{es}. \quad (13)$$

Impedance matrices in rotational task space $M_{\theta e}, B_{\theta e}, K_{\theta e}$ can be approximated from the measured rotational angle of steering wheel $\theta_e(t)$ and steering torque $T_e(t)$, induced by external disturbance, with the least squares method. In dual-arm steering,

$$M_{\theta e}=r^2(M_{es_r}+M_{es_l}) \quad (14)$$

$$B_{\theta e}=r^2(B_{es_r}+B_{es_l}) \quad (15)$$

$$K_{\theta e}=r^2(K_{es_r}+K_{es_l}) \quad (16)$$

where $M_{es_r}, B_{es_r}, K_{es_r}$ describe rotational impedance parameters by the right arm while $M_{es_l}, B_{es_l}, K_{es_l}$ are those by the left arm.

4. Experiments

4.1. Virtual Steering and Shifter

Experiments using the developed driving simulator were conducted under the conditions in **Fig.5**, where viscoelastic patterns were designed to realize the realistic feel of driving in the actual automobile based on the comments of human subjects.

Subjects were asked to manually grasp the steering wheel at specified points (See **Fig.5(c)**), and track the sine wave with amplitude $\pi/6$ rad around 0 rad under fre-

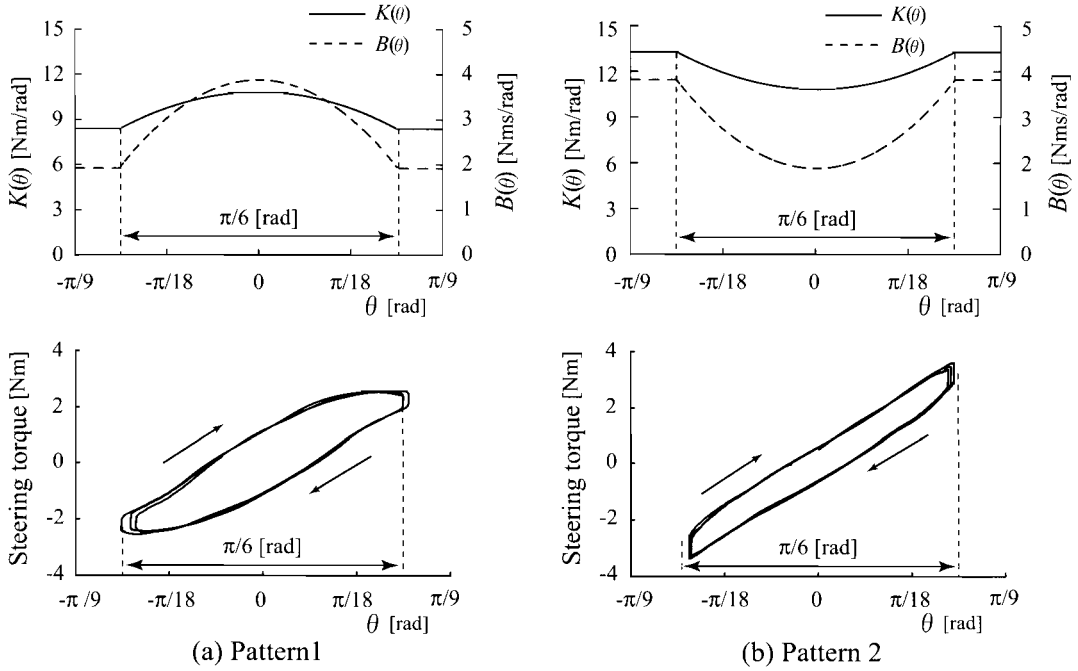

Fig. 6. Operational results for designed viscoelastic patterns in virtual steering.

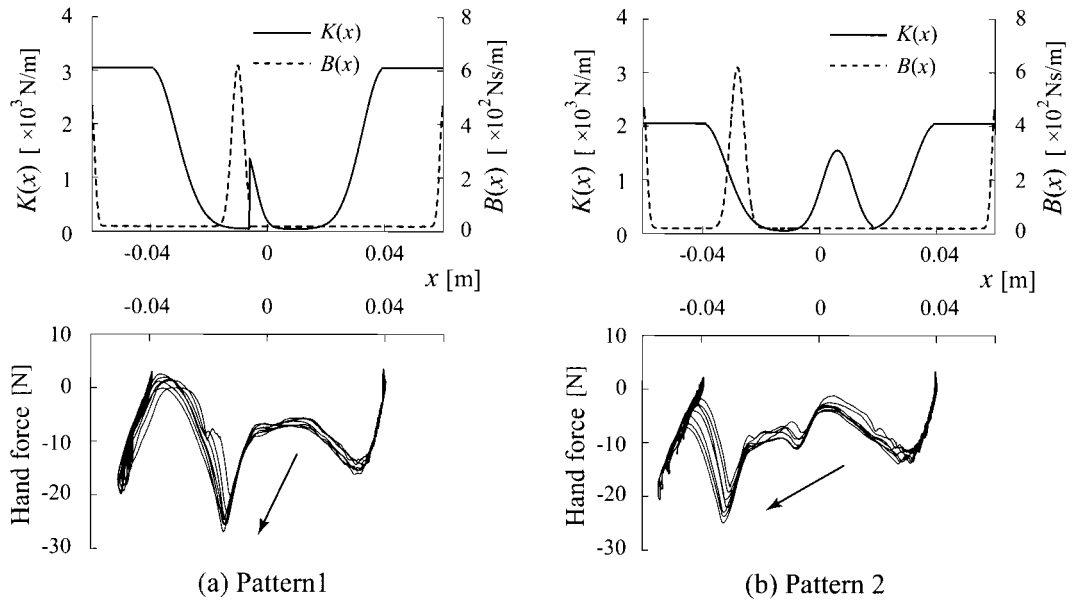

Fig. 7. Operational results for designed viscoelastic patterns in virtual shifting.

quency 0.2Hz using the bio-feedback display in virtual steering. The distance between the subject and steering wheel is determined for each subject in which the relative angle of the elbow joint is set at $\pi/9$ rad. Subjects were asked to move the shifter from Low to 2nd gear after positioning N gear at the specified point in virtual shifting operations (See **Fig.5(b)**). The inertia of the virtual steering wheel was set at $M_\theta = 0.03\text{kgm}^2$, and that of the shifter at $M = 0.45$kg. The distance between the N gear and others was set at 0.04m.

Figure 6 shows viscoelastic patterns in virtual steering and typical examples of torque-to-angle profiles measured during steering. **Fig.7** shows viscoelastic patterns in the virtual transmission shifter and examples of force-to-stroke profiles measured during shifting operations. These experimental results show that the developed driving simulator represents different steering/shifting dynamics by regulating viscoelastic patterns for variable impedance-controlled robots.

4.2. Impedance Measurements by Virtual Steering

Mechanical impedance properties were measured to validate the performance of virtual steering.

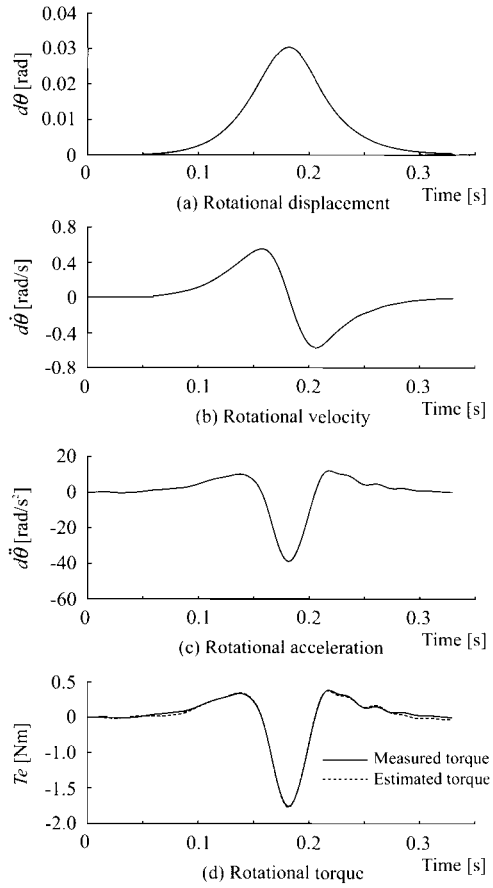

Fig. 8. Example of signals measured during data for estimating mechanical impedance properties.

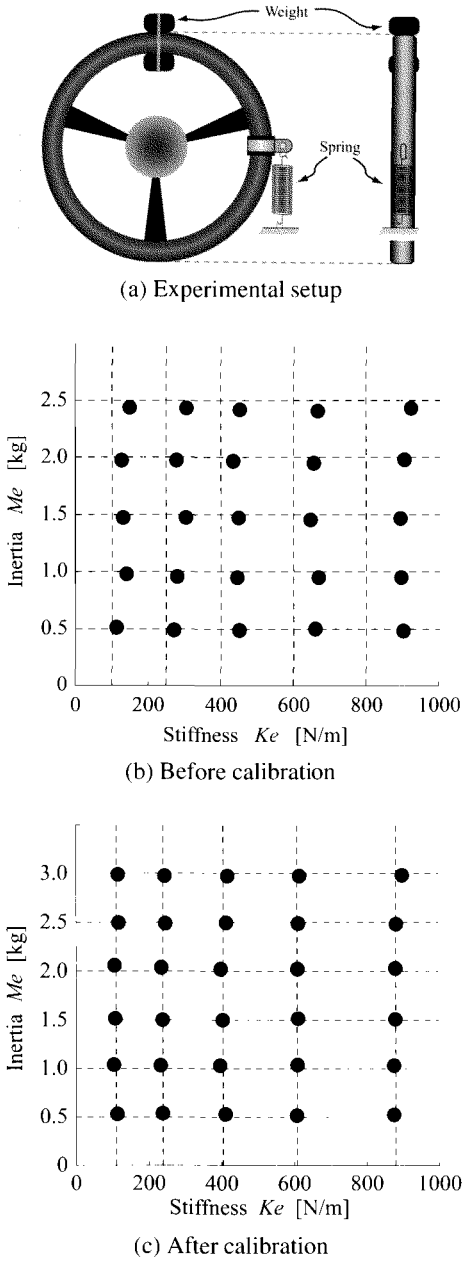

Fig. 9. Accuracy of estimated impedance for known spring-mass system.

Figure 8 shows an example of the measured signal for estimating mechanical impedance properties with a known spring-mass system. **Figs.8(a)**, **(b)**, and **(c)** express time histories of rotational displacement of steering wheel $d\theta(t)$, rotational velocity $d\dot{\theta}(t)$, and rotational acceleration $d\ddot{\theta}(t)$ caused by external disturbance from the top. The solid line in **Fig.8(d)** represents measured steering torque together with estimated torque (dotted line) calculated from Eq.(10), with measured hand movements and estimated hand-impedance parameters. **Fig.8(d)** shows that the steering system accurately estimates mechanical impedance properties because the solid line almost coincides with the dotted one.

Impedance estimation tests for the known spring-mass system were conducted under the experimental setup in **Fig.9(a)**, where a weight was firmly attached to the steering wheel while a spring was set between the steering wheel and the fixed environment. **Fig.9(b)** shows the estimation accuracy before calibration by the developed virtual steering in which steering wheel inertia was removed from estimated values. Means for 5 sets of estimated results are plotted and intersections of dotted lines represent true values of the spring-mass system attached to the steering wheel. Since estimated error on stiffness increased in proportional to desired stiffness as shown in **Fig.9(b)**, values were calibrated with coefficient 0.9016, which is an inverse of the constant of proportionality, to improve estimation accuracy as shown in **Fig.9(c)**. Note that the developed system estimates desired impedance properties successfully.

Measurment tests of human impedance during virtual steering by dual upper arms were conducted for two different positions of the arm wrist (See **Fig.10**). In experiments, a human subject with a driver's license (male university student, aged 22) was asked to grip the steering wheel substantially at specified positions as shown in **Fig.5**. Means and standard deviations of 5 trials for measured impedance properties were as follows: Under the

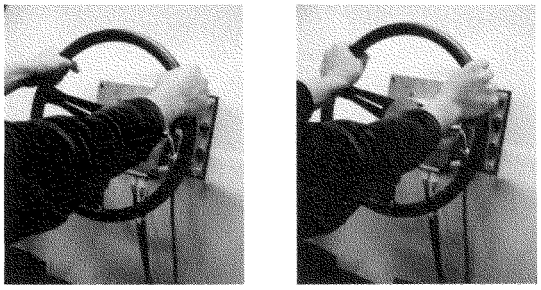

(a) Neutral (b) Extension

Fig. 10. Wrist postures in impedance measurements.

neutral position of the wrist joint, $K_e = 317.25 \pm 53.245$ N/m, $B_e = 63.44 \pm 1.955$ Ns/m, $M_e = 2.52 \pm 0.052$ kg; and under the extended position of the wrist joint, $K_e = 666.44 \pm 107.143$ N/m, $B_e = 50.89 \pm 3.817$ Ns/m, $M_e = 1.75 \pm 0.076$ kg. Stiffness increased since wrist motion is locked by extending the wrist joint as shown in **Fig.10(b)**.

5. Conclusions

The present paper has developed a virtual driving simulator using variable-impedance controlled robots. The simulator provides different operational feelings to human operators by regulating viscoelastic patterns for virtual steering and shifting. It measures mechanical impedance parameters of human multi joint arms tangentially to the steering wheel during virtual steering.

Experiments with the subjects were carried out to validate the effectiveness of the developed simulator by setting the designed viscoelastic patterns that realize realistic feedback in actual drive interfaces. Mechanical impedance properties of the subject were measured according to the rotational angle of the steering wheel.

Future research will be directed to measure mechanical impedance properties of human movements during operations of virtual steering and virtual transmission shifter to develop novel design of robotic systems considering human movements. We also hope to study human impedance properties in the constrained direction important to operating drive interfaces smoothly.

References:

[1] F. A. Mussa-Ivaldi, N. Hogan, and E. Bizzi, "Neural, mechanical and geometric factors subserving arm in humans," Journal of Neuroscience, Vol.5, No.10, pp. 2732-2743, 1985.

[2] J. M. Dolan, M. B. Friendman, and M. L. Nagarka, "Dynamics and loaded impedance components in the maintenance of human arm posture," IEEE Transactions on Systems, Man and Cybernetics, Vol.23, No.3, pp. 698-709, 1993.

[3] T. Tsuji, P. G. Morasso, K. Goto, and K. Ito, "Human hand impedance characteristics during maintained posture," Biological Cybernetics, Vol.72, pp. 457-485, 1995.

[4] T. Tsuji, M. Moritani, M. Kaneko, and K. Ito, "An analysis of human hand impedance characteristics: During isometric muscle contractions," Transaction of the Society of Instrument and Control Engineers, Vol.32, No.2, pp. 271-280, 1996 (in Japanese).

[5] T. Tsuji, Y. Takeda, and Y. Tanaka, "Analysis of mechanical impedance in human arm movements using a virtual tennis system," Biological Cybernetics, Vol.91, No.5, pp. 295-305, 2004.

[6] H. Gomi, Y. Koike, and M. Kawato, "Human hand stiffness during discrete point-to-point multi-joint movement," in Proceedings of the Annual International Conference of IEEE Engineering in Medicine and Biology Society, pp. 1628-1629, 1992.

[7] N. Hogan, "Impedance control: An approach to manipulation," Parts I, II, III, ASME Journal of Dynamic Systems, Measurement, and Control, Vol.107, No.1, pp. 1-24, 1985.

[8] H. Kazerooni, "Human-robot interaction via the transfer of power and information signals," IEEE Transactions on Systems, Man, and Cybernetics, Vol.20, No.2, pp. 450-463, March/April, 1990.

[9] K. Kosuge, Y. Fujisawa, and T. Fukuda, "Control of mechanical system with man-machine interaction," in Proceedings of IEEE International Conference on Intelligent Robots and Systems, pp. 87-92, 1992.

[10] T. Tsuji, Y. Tanaka, and M. Kaneko, "Tracking control properties of human-robot systems," in Proceedings of the 1st International Conference on Information Technology in Mechatronics, pp. 77-83, 2001.

[11] Y. Yamada, H. Konosu, T. Morizano, and Y. Umetani, "Proposal of skill-assist: A system of assisting human workers by reflecting their skills in positioning tasks," Proceedings of the 1999 IEEE International Conference on Systems, Man, and Cybernetics, IV11-16, 1999.

[12] R. Ikeura, and H. Inooka, "Variable impedance control of a robot for cooperation with a human," Proceedings of the 1995 IEEE International Conference on Robotics and Automation, pp. 3097-3102, 1995.

[13] R. Ikeura, T. Moriguchi, and K. Mizutani, "Optimal variable impedance control for a robot and its application to lifting an object with a human," Proceedings of the 2002 IEEE International Workshop on Robot and Human Interactive Communication, pp. 500-505, 2002.

[14] Y. Yamada, H. Daitoh, T. Sakai, and Y. Umetani, "Proposal of a human interface technique for reflecting the operator's intentionality in human/robot collaborative conveyance tasks," Transactions of the Japan Society of Mechanical Engineers, Vol.67, No.665-C, pp. 1069-1076, 2001.

[15] R. Ikeura, H. Hoshino, D. Yokoi et al., "Feeling evaluation for the steering of cars based on impedance of human arm," Proceeding of the SICE System Integration Division Annual Conference, pp. 637-638, 2004.

[16] R. Ikeura, H. Hoshino et al., "Feeling evaluation for the steering of cars based on impedance of human arm," In Proc. of the 2005 JSAE Annual Autom Congress, Society of Automotive Engineers of Japan, pp. 15-20, Sep., 2005.

[17] Y. Tanaka, N. Yamada, K. Nishikawa, I. Masamori, and T. Tsuji, "Manipulability Analysis of Human Arm Movements during the Operation of a Variable-Impedance Controlled Robot," in Proceedings of the 2005 IEEE/RSJ International Conference on Intelligent Robotics and Systems, pp. 3543-3548, August, 2005.

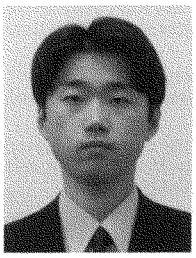

Name:
Yoshiyuki Tanaka

Affiliation:
Department of Artificial Complex Systems Engineering, Hiroshima University

Address:
1-4-1 Kagamiyama, Higashi-hiroshima, Hiroshima 739-8527, Japan

Brief Biographical History:
2001- Research Associate with the Faculty of Information Sciences, Hiroshima City University
2002- Research Associate in the Department of Artificial Complex Systems Engineering at Hiroshima University

Main Works:
• Y. Tanaka, T. Tsuji, V. Sanguineti, and P. G.Morasso, "Bio-mimetic Trajectory Generation using a Neural Time Base Generator," Journal of Robotic Systems, Vol.22, No.11, pp. 625-637, 2005.

Membership in Learned Societies:
• The Robotics Society of Japan
• Institute of Electrical Engineering of Japan
• The Society of Instrumentation and Control Engineers in Japan
• The Institute of Electrical and Electronics Engineers

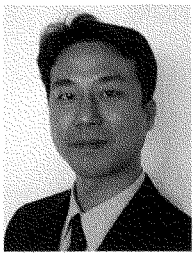

Name:
Naoki Yamada

Affiliation:
Senior Technical Specialist, Technical Research Center, Mazda Motor Corporation

Address:
3-1 Shinchi, Fuchu-cho, Aki-gun, Hiroshima 730-8670, Japan

Brief Biographical History:
1992 Joined Mazda Motor Corporation

Membership in Learned Societies:
• The Japan Society of Mechanical Engineers (JSME)
• Society of Automotive Engineers of Japan (JSAE)
• Japan Ergonomics Society (JES)

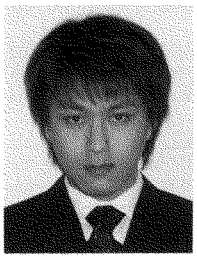

Name:
Ryoma Kanda

Affiliation:
Department of Artificial Complex Systems Engineering, Hiroshima University

Address:
1-4-1 Kagamiyama, Higashi-Hiroshima, Hiroshima 739-8527, Japan

Brief Biographical History:
2001- Faculty of Engineering, Hiroshima University
2005- Graduate School of Engineering, Hiroshima University

Main Works:
• R. Kanda, Y. Tanaka, N. Yamada, K. Fukuba, I. Masamori, and T. Tsuji, "Analysis of human hand impedance properties during the steering operation," Proceedings of the 2005 JSME Conference on Robotics and Mechatronics, No.05-4, 1P1-N-077, pp. 1-2, 2005.

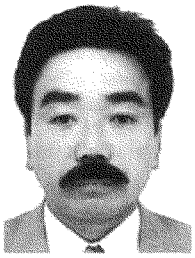

Name:
Hitoshi Fukuba

Affiliation:
Senior Technical Specialist, Technical Research Center, Mazda Motor Corporation

Address:
3-1 Shinchi, Fuchu-cho, Aki-gun, Hiroshima 730-8670, Japan

Brief Biographical History:
1988 Joined Mazda Motor Corporation

Membership in Learned Societies:
• Society of Automotive Engineers of Japan (JSAE)

Name:
Ichiro Masamori

Affiliation:
Senior Research Engineer, Technical Research Center, Mazda Motor Corporation

Address:
3-1 Shinchi, Fuchu-cho, Aki-gun, Hiroshima 730-8670, Japan

Brief Biographical History:
1983 Joined Mazda Motor Corporation

Main Works:
• "Operation analysis using electromyogram measurement technique: application to lift gate closing operation," JSAE Review, Vol.21, pp. 261-263, 2000.

Membership in Learned Societies:
• Society of Automotive Engineers of Japan (JSAE)
• Japan Ergonomics Society (JES)

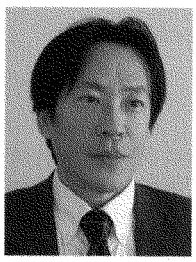

Name:
Toshio Tsuji

Affiliation:
Department of Artificial Complex Systems Engineering, Hiroshima University

Address:
1-4-1 Kagamiyama, Higashi-hiroshima, Hiroshima 739-8527, Japan

Brief Biographical History:
1985- Research Associate in Faculty of Engineering at Hiroshima University
1994- Associate Professor in Faculty of Engineering at Hiroshima University
2002- Professor of Department of Artificial Complex Systems Engineering at Hiroshima University

Main Works:
• T. Tsuji, P. Morasso, K. Goto, and K. Ito, "Human Hand Impedance Characteristics during Maintained Posture in Multi-Joint Arm Movements," Biological Cybernetics, Vol.72, pp. 475-485, 1995.

Membership in Learned Societies:
• The Robotics Society of Japan
• The Japan Society of Mechanical Engineers
• The Society of Instrumentation and Control Engineers in Japan
• The Institute of Electrical and Electronics Engineers